

# LANDMARK: Language-guided Representation Enhancement Framework for Scene Graph Generation

Xiaoguang Chang<sup>1</sup>, Teng Wang<sup>2</sup>, Shaowei Cai<sup>2</sup>  
and Changyin Sun<sup>2,3\*</sup>

<sup>1</sup>School of Cyber Science and Engineering, Southeast University,  
Nanjing, China.

<sup>2\*</sup>School of Automation, Southeast University, Nanjing, China.

<sup>3\*</sup>School of Artificial Intelligence, Anhui University, Hefei, China.

\*Corresponding author(s). E-mail(s): [cysun@seu.edu.cn](mailto:cysun@seu.edu.cn);  
Contributing authors: [xg\\_chang@seu.edu.cn](mailto:xg_chang@seu.edu.cn);  
[wangteng@seu.edu.cn](mailto:wangteng@seu.edu.cn); [shaoweicai@seu.edu.cn](mailto:shaoweicai@seu.edu.cn);

## Abstract

Scene graph generation (SGG) is a sophisticated task that suffers from both complex visual features and dataset long-tail problem. Recently, various unbiased strategies have been proposed by designing novel loss functions and data balancing strategies. Unfortunately, these unbiased methods fail to emphasize language priors in feature refinement perspective. Inspired by the fact that predicates are highly correlated with semantics hidden in subject-object pair and global context, we propose LANDMARK (**LAN**guage-gui**DE**d representation enhance**ME**nt fra**M**ewo**RK**) that learns predicate-relevant representations from language-vision interactive patterns, global language context and pair-predicate correlation. Specifically, we first project object labels to three distinctive semantic embeddings for different representation learning. Then, Language Attention Module (LAM) and Experience Estimation Module (EEM) process subject-object word embeddings to attention vector and predicate distribution, respectively. Language Context Module (LCM) encodes global context from each word embedding, which avoids isolated learning from local information. Finally, modules outputs are used to update visual representations and SGG model's prediction. All language representations are purely generated

from object categories so that no extra knowledge is needed. This framework is model-agnostic and consistently improve performance on existing SGG models. Besides, representation-level unbiased strategies endow LANDMARK the advantage of compatibility with other methods. Code is available at <https://github.com/rafa-cxg/PySGG-cxg>.

**Keywords:** Scene Graph Generation, unbiased method, Vision-language representation learning, Multi-semantics

## 1 Introduction

Scene graph generation (SGG) is a crucial task that benefits image captioning [1, 2], visual question answering [3–5], and video understanding [6]. However, most generated scene graphs faces challenge of trivial predictions, thus far from been applied into practical applications.

Therefore, recent researches have been working on unbiased methods that elevate recall of hardly distinguishable predicates. Generally, unbiased methods can be divided into 3 types: data resampling (e.g., BLS [7], GCL [8]), predicate-aware loss design (e.g., CogTree [9] and FGPL [10]) and logit manipulation (e.g., TDE [11], RTPB [12], FREQ [13]). However, a common drawback is that they rely on explicitly modeling predicate correlations or loss weights from dataset statistics [10, 13] or biased model predictions [10, 11], which means that they are sensitive to prerequisite changes. For instance, [11] is not effective when training on an unbiased model, hence, confining the SGG model performance. Compared with loss and statistic approaches, language representation learning is much robust because it learns implicit patterns of predicates and avoids visual features redundancy, which is not been stressed by unbiased methods before.

However, language representation learning has been adopted by some baseline models. For example, [14] takes word embedding to ground attention on visual features. [8] utilizes Cross Attention (CA) mechanism for multi-modality learning. [15] introduces transformer-based architecture to bridge the gap between images and texts. However, most of these approaches are not plug-and-play, and merely use single language representation regardless of different semantic context. Therefore, failed to unleash power of language.

In fact, words have multiple meaning that carries different priors in terms of different semantics, which can guide scene graph generation. Here, we give a multi-semantic reasoning example in Fig. 1. Given this shopping picture, first, human constructs a predicate distribution by correlation between predicate and the pair *woman-ball* as well as their relative position. This knowledge comes from experience and the process is vision-independent. Next, still based on *woman-ball*, human can build correlation between subject-object pair and visual pattern like “woman’s hand is closed to ball”, which is a strong “holding” relevant pattern. In contrast, woman and girl’s contour are irrelevant in terms

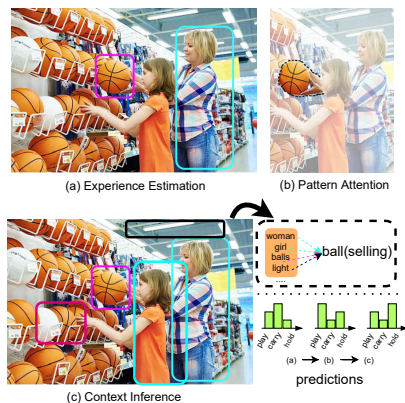


**Fig. 1** An example of multi-semantic language assistance for relation prediction. Bottom-right corner shows 3 candidates’ possibility updating process. a) **Experience Estimation**: human recalls a rough predicate distribution based on co-occurrence possibility of predicates and object pair. b) **Pattern Attention**: using internal relationship between object pair and visual information for locating predicate-relevant visual pattern. c) **Context inference**: using context to refine the meaning of subject and object, preventing prediction biases caused by isolated considering object pairs. The right-bottom shows prediction possibility changing through 3 processes

of this pair. Finally, according to surrounding objects (e.g., balls, girls, lights), human can infer the *selling* context to avoid predicting *play*, because it is not suit in this scene.

Motivated by these observations, we heuristically design 3 plug-and-play language modules that exploit different language prior behind object categories. Three modules take detected object classes as input and generate semantic embeddings into different semantic spaces, which are used for extracting priors from language-visual pattern correlations, language context and pair-predicate correlation, respectively. Concretely, 1) **Language Attention Module** projects subject-object word embeddings to unified semantic matrix, then, channel attention is used to extract attention vector for relation visual feature map, which can learn relevance between object pair and specific predicate-relevant visual patterns 2) **Language Context Module** employs transformer-based encoder to encode the global language context into entity’s semantic embedding from a sequence of entity labels. Comparing with pretrained word embedding, this module can generate semantic representation that fits context. These two modules are used for initializing entity and relation visual-based representations, respectively. 3) **Experience Estimation Module** are supervised by marginal probability of subject-predicate and object-predicate to learn the class and spatial aware predicate distribution as likelihood offset. It is worth mentioning that language processing is disentangled with visual feature at very beginning, so this framework is applicable for most SGG baseline models.

To best of our knowledge, we are the first to utilize multi semantic language representation within object label to achieve unbiased Scene graph generation. The main contributions could be summarized as follows:

1. We propose LANDMARK that introduces language representation learning into unbiased scene graph generation, which stresses the under-explored multiple semantics utilization in object label.
2. We devise three modules that divide object labels into distinctive semantic spaces, then extract priors of language-vision interactive patterns and semantic context as well as pair-predicate correlation, respectively.
3. Experiments on SGG branchmark show constant improvements on baseline models and compatibility with other unbiased methods, which indicate the effectiveness of multi-semantic language representations that induced from object labels.

## 2 Related works

**Scene Graph Generation:** There are mainly two mainstream methods for scene graph generation: Based on context modeling or graph convolutional network (GCN) [16]. The first approach is focused on modeling global information and widely adapted message passing between all entities features [17–21]. A number of them [8, 12, 13, 15, 22] harnessed sequential models e.g., LSTM [23], GRU [24] and Transformer [25]. Chen et al. [12] use two stacks of Transformer to encode global information. Zellers et al. [13] uses LSTM to encode global context that informs relation prediction. However, merely modeling global context is not sufficient for Scene graph tasks. Another approach [7, 26–28] propagate message between node and edge features, and focusing more on regional pair-wise information. [7] applied a multi-stage graph message propagation between proposal entities and relationship representations. In [27], Yang *et al.* pruned graph connections to sparse one, then attentional graph convolution network is applied for modulating information flow. [26] utilized GCN for updating state representations as energy value. Chen *et al.* [29] constructed a graph between proposal and all relationship representations and aggregated messages by GRU. Yet, this approach suffers from insufficient global context encoding. Our method considers both pair-wise and global contexts for representation refinement.

**Language prior learning:** entity labels and relation distributions are most used prior knowledge in scene graph generation. On unbiased method side, language knowledge can be embodied in loss weight or prediction bias. On For example, FREQ [13] directly counts “subject-predicate-object” co-occurrence in dataset as prediction bias. Chen et al. [12] devises different types of specific bias by using different ways to model object relationship from dataset. CogTree [9] proposed a loss based on automatically built cognitive structure of the relationships from the biased SGG predictions. Through mentioned methods get remarkable boost on specific baseline models in terms of metric mRecall@k [30], they are instable when prerequisite changes.

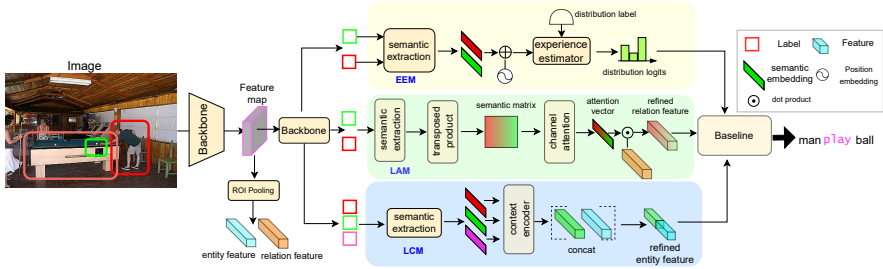


**Fig. 2** LANDMARK architecture. The image first goes through a generic object detector to get predicted object’s label and ROI feature. Then labels are served as three modules input (i.e., EEM, LAM, LCM) and calculated distinctive semantics. Finally, LAM and LCM outputs are used to refine relation and entity representations, respectively. EEM’s output is served as prediction offset.

On the baseline model side, an increasing number of works strived for multi-modality representation learning. [31] designed a language module, which projected representation to the same space of vision module for minimizing the distance of similar semantic features. [30] introduced a confidence estimation module to alleviate the error propagation by incorporating confidence estimation in node feature updating. [32] incorporated external commonsense knowledge by unifying the formulation of scene graph and commonsense graph. [33] structured visual commonsense and proposed a cascaded fusion architecture for fusion. However, existing methods treat language modality as a single representation, which lost a lot of information.

### 3 Methodology

**Problem formulation:** Given an image  $I$ , scene graph generation aims to predict entity class set  $C_e$ , coordination set  $B_e$  and relation set  $C_r$ . Generally, existing SGG models receive visual entity and predicate (or node and edge) representations from backbone. Then a graph  $\mathcal{G} = \{C_e, B_e, C_r\}$  can be formulated.

$$\mathcal{G} = P(C_r, B_e, C_e | I) = SGG(N, E) \quad (1)$$

Where  $N = \{e_i\}_{i=1}^n$  and  $E = \{e_{ij}\}$  are the set of entity and predicate representations. In this paper, we aimed to update  $N$  and  $E$  by incorporating semantic priors.

**Framework overview:** LANDMARK consists of three semantic learning modules, i.e., *Language Attention Module* (LAM), *Language Context Module* (LCM) and *Experience Estimation Module* (EEM). The framework architecture is shown in Fig. 2. First, we obtain  $N$ ,  $E$  from ROI Pooling,  $C_e$ ,  $B_e$  from classifier head. Then, semantic extraction operation convert labels  $\{c_i\}$  to semantic embeddings for each module. For LAM, semantic embeddings of subject  $c_i$  and object  $c_j$  are transposed and multiplied to semantic matrix, then channel attention transfers the matrix to attention vector and

update relation representation. LCM encodes semantic embeddings of all entity labels  $C_e$  presented in the image, generating context-aware semantic entity feature and concatenating it with visual entity representation. The updated entity and relation representation are passing through the baseline model. For EEM, the distribution label is generated to supervise experience estimator, which combine subject-object semantic embedding with position embedding to yield distribution logits. Finally, generated logits are used to update the final predicate likelihood.

### 3.1 Semantic extraction

Semantic extraction is used to transfer labels to the corresponding semantic space, which is applied on three modules independently. Specifically, semantic extractor consists of three operations:

$$\begin{aligned} f_{se}^{sub}(c_i) &= w_s^T c_i \\ f_{se}^{obj}(c_j) &= w_o^T c_j \\ f_{se}^{ent}(c_e) &= w_e^T c_e \end{aligned} \quad (2)$$

The first and second operations are used in LAM and EEM for subject and object projection respectively. Considering that the same word as subject or object may have contrastive meaning (e.g., *eating* could be a possible predicate if “man” is subject, which is impossible when “man” is object), we use different weights  $w_s$  and  $w_o$  to project subject and object to semantic embedding. Last operation is used in LCM, since all labels are treated as objects, we use unified  $w_e$  as semantic embedding weight.

In fact,  $f_{se}$  could be any projection function as long as the input is object labels. Here, we only use a naive 1-layer linear function to prove the extraction’s effectiveness.

### 3.2 Language Attention Module

This module aims to learn the prior between object pair and visual predicate-relevant patterns within visual relation representation  $e_{ij}$ . Original feature extraction network (e.g., Reset [34]) keep both spatial and semantic information. Specially, different channels focus on different visual patterns. However, relation visual feature inevitably mix up with huge amount of irrelevant background information, so there is a need for channel selection. Heuristically, given a specific subject-object pair (e.g., *boy-basketball* or *boy-street*), visual feature should have different activation. Therefore, we design a label-aware channel attention mechanism. Specifically, given subject  $i$  and object  $j$ , we first generate a semantic matrix  $x_{ij}$  as a unique representation of word-vision correlation.

$$x_{ij} = f_{se}^{sub}(c_i) \otimes f_{se}^{obj}(c_j)^T \quad (3)$$

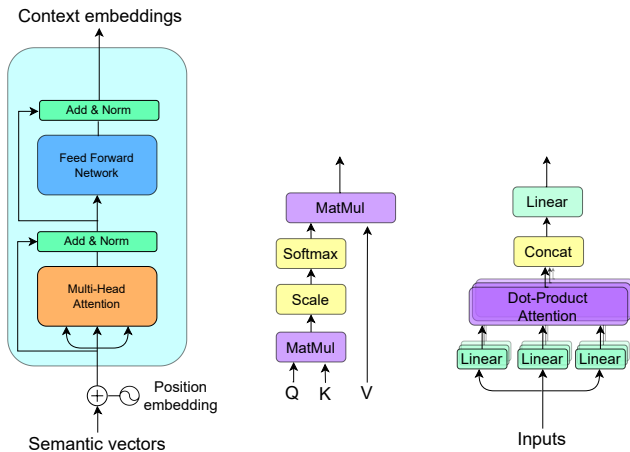


**Fig. 3** Context Encoder block structure (left). Dot-Product Attention (middle). Multi-Head Self Attention (right).

Where  $\otimes$  refers to matrix multiplication. We achieve channel attention by a series of 2D convolutions with the spatial pooling on  $x_{ij}$  to get attention vector  $e_{ij}^c$ :

$$e_{ij}^c = \sigma(G_{\text{pooling}}(G_{\text{conv}}^{n_c} \dots \sigma(G_{\text{conv}}^1(x_{ij})))) \in \mathcal{R}^{C,1} \quad (4)$$

Where  $C$  is as the channel number of visual relation feature  $e_{ij}$ ,  $n_c$  is the number of 2D convolution layers,  $G_{\text{pooling}}$  is pooling operation,  $\sigma$  is activation function. Finally, the channel weights  $e_{ij}^c$  will be used for updating  $e_{ij}$ , so that irrelevant channel for relation discrimination will be suppressed.

$$\hat{e}_{ij} = e_{ij} \times e_{ij}^c \quad (5)$$

Where  $\hat{e}_{ij}$  is refined relation representation,  $\times$  is dot product operator.

### 3.3 Language Context Module

Compared with visual information, single word is semantically isolated from other components in a sentence. Though we devise LAM and EEM for semantic extraction, the utilized pairwise labels are confined to local semantics, which is insufficient for comprehensive semantic inference. Hence, LCM is aiming at addressing the global context deficiency problem. This module includes semantic extractor and context encoder. The context encoder consists of multilayer transformer encoder with Multi-Head Self-Attention (MHSA) [25] and Feed Forward Network (FFN) [25]. The structure is illustrated in Fig. 3. Concretely, given an image, supposed there are  $n$  entities, the input sequence  $X$  could be described as follows:

$$X = \{s_0, s_1, \dots, s_n\} \quad (6)$$

where

$$s_i = \gamma(f_{se}^e c_i + p_i) \in \mathbb{R}^d \quad (7)$$

Here,  $c_i$  and  $p_i = \phi[x_i, y_i, w_i, h_i]$  refer to class labels and entity's position embedding of the  $i$ -th entity.  $x_i, y_i, w_i, h_i$  are center coordinates, width, height of the object  $i$ .  $\gamma$  denotes the learnable linear transformation. Where  $d$  is the dimension of each element in the sequence. We first reiterate standard Scaled Dot-Product Attention [25].

$$\text{Attention}(Q, K, V) = \text{softmax}\left(\frac{QK^T}{\sqrt{d_k}}\right)V \quad (8)$$

Then, Multi-Head Self Attention is formulated as:

$$\begin{aligned} \text{MHSA}(X) &= \text{Concat}(\text{head}_1, \dots, \text{head}_h)W^O \\ \text{head} &= \text{Attention}\left(XW_i^Q, XW_i^K, XW_i^V\right) \end{aligned} \quad (9)$$

Where  $W_i^Q, W_i^K, W_i^V$  and  $W^O$  are parameter matrices. The  $b$ -th layer output  $X_b$  can be denoted as:

$$X'_b = \text{MHSA}(\text{LN}(X_{b-1})) + X_{b-1}, \quad (10)$$

$$X_b = \text{FFN}(\text{LN}(X'_b)) + X'_b, \quad (11)$$

Where  $X_{b-1}$  is the  $(b-1)$ th layer, and we set  $X_0 = X$ . LN is layer normalization. Differing from previous works [35][12], LCM takes a sequence of entity labels as inputs, so module can learn semantic entity representation on top of high level information.

### 3.4 Experience Estimation Module:

This module is deigned to supervised learn the relationship distribution prior from subject-object pair, as a compensation of cross entropy loss. EEM consists of semantic extractor, experience estimator and distribution label generation for supervision. Since entity class and position both have influence on judging relation, This module utilizes both classes and position information to learn precise distribution. First, we embed entity label  $i, j$  and position embedding  $p_{ij}$  to high dimension representation space, then, experience estimator predict the predicate distribution  $d_{ij}$  between subject  $i$  and object  $j$ .

$$p_{ij} = \phi_p[x_i, y_i, w_i, h_i, x_j, y_j, w_j, h_j] \quad (12)$$

$$d_{ij} = \varphi[\phi_s(f_{se}^{sub}(c_i))\phi_o(f_{se}^{obj}(c_j)), p_{ij}] \quad (13)$$

Where  $[\cdot, \cdot]$  refers to concatenation operation,  $\phi_p, \phi_s, \phi_o, \varphi$  are fully connected layers with RELU as activation function. Finally, we merge relationship distribution  $d_{ij}$  with the prediction from the baseline, which could be described as follows:

$$\hat{d}_{i,j} = \text{SGG}(\hat{n}_{ij}, \hat{e}_{ij}) + d_{ij} \quad (14)$$

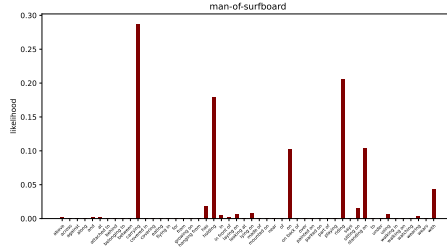


**Fig. 4** Joint possibility for subject *man* and object *surfboard*. The groundtruth triplet  $\langle \text{man}, \text{of}, \text{surfboard} \rangle$  is sampled from zero-shot split (where triplets are only in evaluation set but not occurred in training set).

Where  $\hat{d}_{i,j}$  is the updated prediction likelihood.  $\hat{n}_{ij}$  and  $\hat{e}_{ij}$  are enhanced entity and relation feature obtained by LAM and CAM (Section 3.2, 3.3).

**Distribution label generation:** Dataset annotations are inherently reflect human commonsense, so we manage to generate accurate distribution labels from dataset. For subject  $i$ , object  $j$ , we obtain  $m_i^{sub}$   $m_j^{obj}$  as “subject-predicate” and “predicate-object” marginal distributions. Since  $m_i^{sub}, m_j^{obj}$  are independent distribution, we calculate joint possibility  $p_{ij}^{joint}$  as followed:

$$p_{ij}^{joint} = m_i^{sub} \odot m_j^{obj} \quad (15)$$

Where  $\odot$  denotes the element-wise product. Though EEM is alike FREQ [13] that generating predicate distribution from statistics, FREQ directly counts triplets  $\langle \text{subject}, \text{predicate}, \text{object} \rangle$  occurrence. However, some triplet samples are scarce in training samples, so it is hard to establish an informative distribution prior. In contrast, EEM uses joint possibility as labels to infer the predicate distribution. Fig. 4 is a typical example of generated joint possibility  $p_{ij}^{joint}$  of a triplet that not occurred in training set. In this circumstance, FREQ could not work due to zero sample number, whereas, we can see that top 5 highest likelihoods are reasonable and include many possible scenarios. In contrast, the predicate “of” is ambiguous. Better predicate could be one of top likelihoods from joint possibility.

Considering that introducing position information makes accurate predicate possible, we design a fusion function for mitigating joint possibility and true predicate label. The distribution label  $l_{ij}$  can be denoted as:

$$l_{ij} = \mu \times p_{ij}^{joint} + (1 - \mu) \times \text{onehot}[r_{ij}] \quad (16)$$

Where  $\mu$  is a factor regulating proportion of marginal frequency.  $r_{ij}$  refers to real predicate label between subject  $i$  and object  $j$ .

**Objective function:** we choose MSE loss between distribution label  $l_{i,j}$  and predicted distribution  $d_{i,j}$ , which is denoted as:

$$\text{MSE} = \frac{1}{K} \sum_{i=1}^K (d_i, l_i)^2 \quad (17)$$

Where K is the number of relation categories in dataset.

### 3.5 Baseline Model

Any off-the-shelf two-stage scene graph generation model can be used as baseline. It could be either a sequential model or a graph neural network, as long as it exerts entity and relation features for prediction.

## 4 Experiments

In this section, we first introduce the experiment settings in our experiments. Then, we test our framework’s effectiveness on several SGG models, and conduct experiment to analyze the compatibility between our method and the state-of-art unbiased strategies. Finally, detailed analyzations and quantitative evaluations are presented to further verify LANDMARK in different perspectives.

### 4.1 Experiment settings

**Datasets** We employ the widely adopted Visual Genome [36] filtered sub-dataset VG150 [37] to train and evaluate our framework. The VG150 dataset contains the most frequent 150 object categories and 50 predicate categories in VG. It consists of more than 108k images, with 70% images held out for training and 30% for testing. Among the training set, 5000 images are used for evaluation.

**Tasks.** We consider three conventional sub-tasks of scene graph generation to evaluate our framework. 1) *Predicate Classification (PredCls)* predicts relationships between each object pairs given their ground-truth bounding boxes and classes. 2) *Scene Graph Classification (SGCls)* predicts the object classes and their relationships given the ground-truth bounding boxes of objects. 3) *Scene Graph Detection (SGDet)* needs to detect object classes, bounding boxes and predict their relationships.

**Evaluation Metrics** we report widely accepted metrics Mean Recall@k [29] and Recall@k [30] for evaluating models performance. Recall@k computes the fraction of times the correct relationship is predicted in the top k relationship predictions. However, the R@K fails to reflect the performance on tail relationship categories, thus, Recall on each class (i.e., mean Recall) is used to evaluate unbiased performance. Besides, In order to evaluate EEM, we need a metrics to measure distribution accuracy, so that TOP-N Recall@K metric are

purposed by allowing top N scored predicate in one prediction as candidates, then,  $N \times K$  number of candidates are used for calculating Recall, i.e.

$$\text{TOP-N Recall@K} = \frac{\text{correct}(\{\text{candidates}\}_{N \times K})}{N_{gt}}$$

When  $N=1$ , TOP-N Recall@K is equal to Recall@K. The difference between TOP Recall and Recall with no graph constraint [38] is the former one forcing top  $N \times K$  scored predicates to be preserved, avoiding candidates been excluded by higher scored in other predictions.

**Implementation Details** We use pretrained Faster R-CNN [39] with backbone ResNeXt-101-FPN [40] and ROIAlign [40] as object detector. We froze its weights during training. For our framework, we use pretrained GloVe [41] weight as initial  $w_s, w_o, w_e$  in semantic extractor. For EEM, we use 3 layers MLP  $\Phi_s, \Phi_o, \Phi_p$  with 1024 neurons,  $\varphi$  is a 2 layers MLP with hidden dimension 4096.  $\mu$  referred in Eq. 16 are set to 0.3 for unbiased methods, 0.7 for baseline models. For Eq. 4, we choose two  $3 \times 3$  convolution layers to generate a 256-channel attention vector. For LCM, We choose context encoder with 4 layers and 8 heads, entity dimension  $d = 512$ . For training, approximately 10000 iterations is enough for each baseline. The basic learning rate is 0.01 and batch size is 16. We choose the SGD optimizer for optimization.

## 4.2 Comparison with baseline methods

Table 1 shows mRecall & Recall of 5 baseline models with or without our framework LANDMARK. Baseline models include GCN based models: G-RCNN [27], BGNN [7] and context modeling networks: IMP [37], Transformer [25], Motifs [13]. It is worth mentioning that we do not deploy any unbiased strategies on these models. We observe that incorporating our proposed LANDMARK leads to a consistent mRecall improvement in all three tasks for all baseline models, which demonstrates the robustness of our approach. For mR@100, our model average improvements are 3.66%, 2.64%, 1.37% on three tasks. The improvements might be attributed to the fact that multi-semantic language representation indeed facilitates visual representation. It is not surprised that average improvement consecutively shrinks in three tasks, due to inaccurate class and position predicted by pretrained object detector. Besides, Recall shows drops in different extent, which is a common characteristic of an unbiased method.

We also measure the total parameter amounts (M) and computation overhead (GFLOPs) of baseline and LANDMARK in Table 1. Generally, there is 20M (relative: 5.3%) parameters and 2.5GFLOPs (relative: 1.0%) computation increased. In comparison with BGNN+TDE (365.7M & 213.2GFLOPs), both model size and computation overhead are smaller. That is attributed to lightweight module design and adoption of low-dimensional inputs (i.e., language rather than image inputs.)

**Table 1** The SGG performances of mRecall & Recall on VG dataset in %. \* denotes the default unbiased strategy in paper is not applied. All baselines are reimplemented on our codebase.

Model	Method	PredCls		SGCls		SGDet		Params(M)/GFLOPs
		mR@50/100	R@50/100	mR@50/100	R@50/100	mR@50/100	R@50/100	
IMP [37]	baseline	16.88/18.02	66.8/68.25	7.57/8.08	38.9/40.17	6.00/7.30	27.24/34.24	336.3/206.4
	LANDMARK	<b>19.54/21.06</b>	64.89/66.61	<b>9.89/10.49</b>	33.63/34.89	<b>6.47/8.00</b>	24.34/29.05	356.5/208.8
Transformer [25]	baseline	19.13/20.3	65.59/67.21	10.25/10.72	39.3/40.5	7.99/9.68	26.91/31.26	330.6/205.6
	LANDMARK	<b>22.19/23.87</b>	65.48/66.92	<b>11.94/12.84</b>	36.62/37.73	<b>8.23/10.43</b>	<b>28.76/32.70</b>	348.5/207.8
G-RCNN [27]	baseline	16.46/17.28	66.27/67.9	9.67/10.17	39.3/40.5	4.89/5.95	30.37/34.47	366.1/207.1
	LANDMARK	<b>19.24/20.51</b>	65.76/67.50	<b>11.14/11.62</b>	<b>42.80/43.55</b>	<b>5.52/7.21</b>	24.61/29.69	386.4/209.6
Motifs [13]	baseline	18.79/19.69	66.17/67.72	9.39/9.97	41.57/42.7	6.24/7.54	29.82/33.65	367.1/211.5
	LANDMARK	<b>22.37/23.79</b>	59.34/61.16	<b>14.36/15.25</b>	33.57/35.02	<b>7.87/10.56</b>	24.65/28.87	389.8/214.4
BGNN [7]	baseline	17.26/18.29	66.14/67.65	10.30/10.83	39.94/41.17	6.46/8.22	30.90/35.36	341.9/205.0
	LANDMARK	<b>20.35/22.63</b>	55.10/57.16	<b>11.64/12.79</b>	33.3/34.89	<b>7.34/8.97</b>	24.34/29.05	360.1/207.2

### 4.3 Compatibility with unbiased methods

The most tricky problem of unbiased SGG strategies is that most of them has demanding application case. Hence, we test our framework’s compatibility with other unbiased methods by stacking two methods together, the mRecall & Recall are listed in Table 2. The listed strategies belong to different type, e.g., Data re-sampling: BLS [7], logit manipulation: e.g. TDE [11], and feature refinement: LANDMARK (ours). According to this table, there are several findings:

- Applying LANDMARK with other methods is worked. For instance, BLS with LANDMARK on BGNN get new SOTA performance. The reason has two: 1) LANDMARK has distinctive semantic feature enhancement strategy, which do not conflict with other methods. 2) Most of unbiased methods are designed to obtain priors from biased prerequisites (e.g., baseline, long-tailed dataset), whereas LANDMARK is baseline-independant, that is, baseline do not affect LANDMARK’s inference.
- Only a tiny improvement, or even decrease in mR@K occurred when using BLS and TDE together. For example, Motif+BLS+TDE results in obvious decrease in mR@k. This suggests that these methods are sensitive to changes of external circumstances (e.g., sampling distribution, baseline model capability).
- Our network do not sacrifice Recall a lot. For example, BLS+LANDMARK on Motifs has higher Recall than without LANDMARK. However, using BLS+TDE remarkably impair the Recall performance. We speculate that existing unbiased methods do not explore real discrepancies between predicates, but only on increasing likelihood of tail predicates.

### 4.4 Analyze Each Predicate:

Shown in Fig. 5, we present VG dataset’s class distribution and Recall@100 improvements on Predcls task (BGNN+BLS w/ or w/o ours). Over all 50 predicates, only 11 predicates predicted by baseline are superior to LANDMARK. Besides, there are 6 hard-to-distinguish predicates (i.e. *bitam*, *belong to*, *walking on*, *mounted on*, *made of*, *says*) are recalled by LANDMARK.

**Table 2** Compatibility test of unbiased methods and LANDMARK in %. \* means this Baseline model and unbiased method are proposed in the same paper. All methods are reimplemented on our codebase.

Method	PredCls		SGCls		SGDet	
	mR@50/100	R@50/100	mR@50/100	R@50/100	mR@50/100	R@50/100
Motifs <sub>TDE</sub>	22.87/25.90	35.28/41.11	13.76/15.36	23.88/27.42	7.87/9.55	9.83/13.06
Motifs <sub>BLS</sub>	30.64/32.76	54.56/56.27	20.21/21.09	34.11/35.00	13.20/15.97	25.27/28.88
Motifs <sub>BLS+TDE</sub>	26.19/30.84	17.01/18.89	17.31/19.28	19.63/21.43	9.18/11.89	8.34/10.27
Motifs <sub>TDE+LANDMARK</sub>	24.59/29.27	39.24/45.25	14.43/17.03	28.70/32.28	8.98/11.35	9.92/12.85
Motifs <sub>BLS+LANDMARK</sub>	<b>33.62/35.69</b>	<b>55.29/56.80</b>	<b>21.43/22.05</b>	<b>36.02/36.85</b>	<b>13.86/16.31</b>	<b>25.10/29.12</b>
BGNN <sub>TDE</sub>	19.23/21.59	32.75/36.45	13.09/14.18	28.66/31.20	8.65/11.01	20.36/26.00
BGNN <sub>BLS</sub>	30.64/32.76	55.39/56.8	16.69/17.83	35.70/36.94	13.17/15.56	23.54/27.56
BGNN <sub>BLS+TDE</sub>	31.88/34.89	30.37/33.33	16.97/18.70	21.62/23.52	11.60/14.32	19.45/24.11
BGNN <sub>TDE+LANDMARK</sub>	20.32/22.78	50.21/53.85	14.56/15.58	35.31/ <b>37.38</b>	9.68/12.41	<b>25.72/27.98</b>
BGNN <sub>BLS+LANDMARK</sub>	<b>34.41/36.43</b>	53.99/55.42	<b>18.27/19.12</b>	34.55/35.80	<b>14.08/18.34</b>	24.87/ <b>29.41</b>

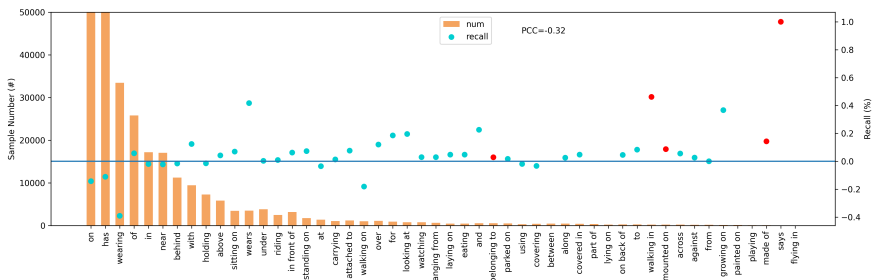


**Fig. 5** Data sampling distribution and Recall@100 improvements of LANDMARK on BGNN+BLS over each predicate (on Predcls task). The red dots indicate BGNN+BLS failed to. PCC is abbreviation of Pearson Correlation Coefficient

For exploring correlation of Recall improvements and data distribution, Pearson Correlation Coefficient (PCC) is used. PCC=0.32 shows weak negative correlation between dataset bias and LANDMARK improvements. Needed to be noticed that some unbiased methods oversampling tail classes, so that reveal strong negative correlation (e.g., TDE: PCC=-0.56). Besides, PCC between data distribution and LANDMARK or BLS on BGNN (-0.1 vs -0.3) proves both improvements and predictions are robustness to long-tail data.

## 4.5 Ablation Studies

We investigate each LANDMARK component by incrementally adding EEM, LAM, LCM to the BGNN+BLS. The results in Table 3 indicate that: 1) each component are helpful for the whole framework, and no confliction between them. It proves three modules extract distinctive semantics from same label inputs. 2) EEM module mainly improves Predcls than other tasks, which might caused by less accurate position and object label predictions. 3) LCM and LAM consistently promote performances of each task. Because priors from language context and correlation of word-visual patterns are relatively robust to misclassified but closed semantic object labels.

**Table 3** Ablation studies on framework structure in three tasks

Methods			PredCls	SGCls	SGDet
EEM	LAM	LCM	mR@50/100	mR@50/100	mR@50/100
			30.64/32.76	16.69/17.83	13.17/15.56
✓			31.75/33.00	17.27/18.18	13.54/15.92
✓	✓		32.06/33.36	17.75/18.89	14.34/16.42
	✓	✓	34.10/36.07	18.07/19.01	13.89/17.00
✓	✓	✓	<b>34.41/36.43</b>	<b>18.27/19.12</b>	<b>14.08/18.34</b>

**Table 4** EEM module and FREQ model comparison on baseline Motifs.

Method	Predcls	SGCls	SGDet
	Top 1/5 R@100	Top 1/5 R@100	Top 1/5 R@100
FREQ [13]	14.72/ <b>42.47</b>	9.71/27.56	7.66/18.32
EEM	<b>22.74</b> /40.38	<b>14.76</b> / <b>29.14</b>	<b>14.13</b> / <b>23.43</b>

## 4.6 Analyzation of Experience Estimation module:

Mentioned before, Language Attention Module independently outputs predicate predictions, which is alike Frequency Baseline (FREQ) [13]. Therefore, we evaluate EEM and FREQ trained on BGNN+BLS+LANDMARK on evaluation dataset split, results are in Table 4. Except Top-5 on Predcls task, all performance of EEM are outperformed FREQ, and the gap enlarged along with task difficulty increased. It is attributed to supervision from marginal possibility that alleviates the deficiency of rare subject-object sample. Besides, position information introduced in EEM make it accurate when inferencing same object pair.

## 4.7 Analyzation of Language Attention Module:

To validate LAM module’s effectiveness, we visualize heatmap of relation representation  $\hat{e}_{ij}$  (Eq. 5) trained on BGNN+BLS+LANDMARK with true or random generated subject-object pair (with red words) in Figure 6. Intuitively, we can notice that attention area is correlated with given subject and object. For instance, in the leftmost two images, attention area transfers from foot to middle of man’s body when object changes from *shoe* to *shirt*. While given irrelevant words in rightmost two images, e.g., *clock-snow*, module seems to interest in top left and bottom area, which suggest LAM can associate words to related visual pattern without given coordinates.

## 4.8 Evaluation of EEM factor

Fig. 7 shows 4 model’s results of mRecall@100 on SGDet task with different EEM’s factor  $\mu$  in Eq. 16. We find that for baseline models, factor=0.7 is preferable, for unbiased methods, 0.3 is better. This indicates that calculated marginal probability mainly records diversified possible predicates, whereas real labels are more likely to be head predicates.

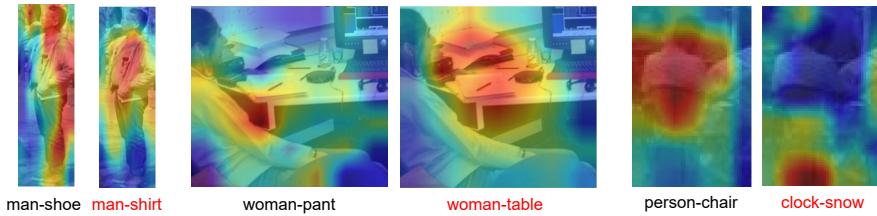


**Fig. 6** Evaluation of LAM. We visualize union area by given groundtruth subject-object pair and random generalized pair (red words), which shows connection between word pair and particular visual features.

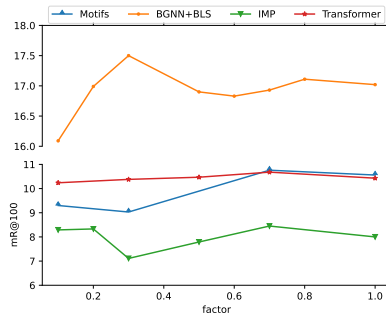


**Fig. 7** mR@100 performance of SGG models with different EEM's factor on SGGDet task.

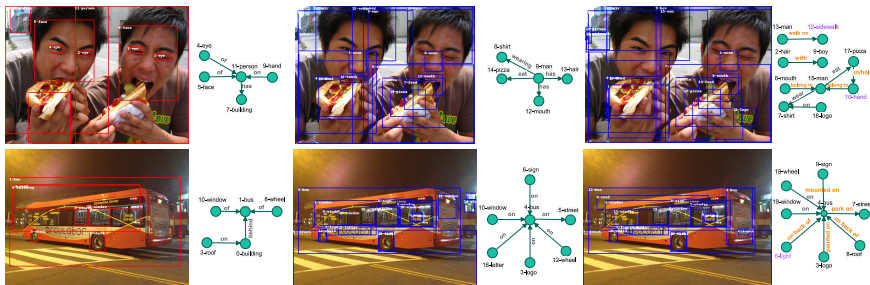


**Fig. 8** Visualization Results: we present scene graphs generated by annotations, BGNN with BLS (unbiased model) and LANDMARK in three columns, respectively. The relations and entities that neither occur in annotations nor baseline are marked with purple and orange.

## 4.9 Qualitative studies

We visualize scene graph generation result from annotations, BGNN with BLS (unbiased model), and BGNN+BLS+LANDMARK on Predcls task in Fig. 8. Intuitively, annotations and unbiased model tends to predict relationships between “less informative pairs” (e.g., *person-eye*, *roof-building* and *light-bus*) that pretty conventional. LANDMARK can further detect relationships between *man-sidewalk* or *roof-bus*. Besides, LANDMARK focuses on

high semantic and positional relationships. For instance, “hand hold pizza” and “light-on back of-bus”, which prove that our framework successfully learns position relationship between objects.

## 5 Conclusion

In this paper, we first point out inadequate language modality utilization in precious SGG methods. Therefore, motivated by language’s polysemy, we purpose a representation enhancement framework (LANDMARK) for SGG task, featured by multi semantic extraction from object labels. This plug-in network explores word-vision correlated pattern and language context from word embedding, and learns predicate distribution from subject-object pair with position. Compared with other unbiased methods, our framework is a new approach from representation refinement perspective. Experiment and analyzes shows constant improvement on Baseline models and compatibility on other unbiased methods.

## Declarations

### Competing interests:

No potential conflict of interest was reported by the authors

### Availability of data and materials:

The data that support the findings of this study are available on request from the first author. The results can be implemented by our GitHub repo.

### Code availability:

The code are openly available in [PySGG-cxg] at [<https://github.com/rafa-cxg/PySGG-cxg>].

## References

- [1] Gu, J., Joty, S., Cai, J., Zhao, H., Yang, X., Wang, G.: Unpaired image captioning via scene graph alignments. In: Proceedings of the IEEE/CVF International Conference on Computer Vision, pp. 10323–10332 (2019)
- [2] Xu, N., Liu, A.-A., Liu, J., Nie, W., Su, Y.: Scene graph captioner: Image captioning based on structural visual representation. *Journal of Visual Communication and Image Representation* **58**, 477–485 (2019)
- [3] Zhang, C., Chao, W.-L., Xuan, D.: An empirical study on leveraging scene graphs for visual question answering. arXiv preprint arXiv:1907.12133 (2019)

- [4] Shi, J., Zhang, H., Li, J.: Explainable and explicit visual reasoning over scene graphs. In: Proceedings of the IEEE/CVF Conference on Computer Vision and Pattern Recognition, pp. 8376–8384 (2019)
- [5] Teney, D., Liu, L., van Den Hengel, A.: Graph-structured representations for visual question answering. In: Proceedings of the IEEE Conference on Computer Vision and Pattern Recognition, pp. 1–9 (2017)
- [6] Teng, Y., Wang, L., Li, Z., Wu, G.: Target adaptive context aggregation for video scene graph generation. In: Proceedings of the IEEE/CVF International Conference on Computer Vision, pp. 13688–13697 (2021)
- [7] Li, R., Zhang, S., Wan, B., He, X.: Bipartite graph network with adaptive message passing for unbiased scene graph generation. In: Proceedings of the IEEE/CVF Conference on Computer Vision and Pattern Recognition (CVPR), pp. 11109–11119 (2021)
- [8] Dong, X., Gan, T., Song, X., Wu, J., Cheng, Y., Nie, L.: Stacked hybrid-attention and group collaborative learning for unbiased scene graph generation. arXiv preprint arXiv:2203.09811 (2022)
- [9] Yu, J., Chai, Y., Wang, Y., Hu, Y., Wu, Q.: Cogtree: Cognition tree loss for unbiased scene graph generation. arXiv preprint arXiv:2009.07526 (2020)
- [10] Lyu, X., Gao, L., Guo, Y., Zhao, Z., Huang, H., Shen, H.T., Song, J.: Fine-grained predicates learning for scene graph generation. In: Proceedings of the IEEE/CVF Conference on Computer Vision and Pattern Recognition, pp. 19467–19475 (2022)
- [11] Tang, K., Niu, Y., Huang, J., Shi, J., Zhang, H.: Unbiased scene graph generation from biased training. In: Proceedings of the IEEE/CVF Conference on Computer Vision and Pattern Recognition, pp. 3716–3725 (2020)
- [12] Chen, C., Zhan, Y., Yu, B., Liu, L., Luo, Y., Du, B.: Resistance training using prior bias: toward unbiased scene graph generation. arXiv preprint arXiv:2201.06794 (2022)
- [13] Zellers, R., Yatskar, M., Thomson, S., Choi, Y.: Neural motifs: Scene graph parsing with global context. In: Proceedings of the IEEE Conference on Computer Vision and Pattern Recognition, pp. 5831–5840 (2018)
- [14] Gkanatsios, N., Pitsikalis, V., Koutras, P., Maragos, P.: Attention-translation-relation network for scalable scene graph generation. In: Proceedings of the IEEE/CVF International Conference on Computer Vision Workshops, pp. 0–0 (2019)

- [15] Zhong, Y., Shi, J., Yang, J., Xu, C., Li, Y.: Learning to generate scene graph from natural language supervision. In: Proceedings of the IEEE/CVF International Conference on Computer Vision, pp. 1823–1834 (2021)
- [16] Kipf, T.N., Welling, M.: Semi-supervised classification with graph convolutional networks. arXiv preprint arXiv:1609.02907 (2016)
- [17] Lin, X., Ding, C., Zeng, J., Tao, D.: Gps-net: Graph property sensing network for scene graph generation. In: Proceedings of the IEEE/CVF Conference on Computer Vision and Pattern Recognition, pp. 3746–3753 (2020)
- [18] Wang, W., Wang, R., Shan, S., Chen, X.: Exploring context and visual pattern of relationship for scene graph generation. In: Proceedings of the IEEE/CVF Conference on Computer Vision and Pattern Recognition (CVPR) (2019)
- [19] Woo, S., Kim, D., Cho, D., Kweon, I.S.: Linknet: Relational embedding for scene graph. Advances in Neural Information Processing Systems **31** (2018)
- [20] Li, Y., Ouyang, W., Zhou, B., Shi, J., Zhang, C., Wang, X.: Factorizable net: an efficient subgraph-based framework for scene graph generation. In: Proceedings of the European Conference on Computer Vision (ECCV), pp. 335–351 (2018)
- [21] Liu, Y., Wang, R., Shan, S., Chen, X.: Structure inference net: Object detection using scene-level context and instance-level relationships. In: Proceedings of the IEEE Conference on Computer Vision and Pattern Recognition, pp. 6985–6994 (2018)
- [22] Li, Y., Ouyang, W., Zhou, B., Wang, K., Wang, X.: Scene graph generation from objects, phrases and region captions. In: Proceedings of the IEEE International Conference on Computer Vision, pp. 1261–1270 (2017)
- [23] Hochreiter, S., Schmidhuber, J.: Long short-term memory. Neural computation **9**(8), 1735–1780 (1997)
- [24] Cho, K., Van Merriënboer, B., Gulcehre, C., Bahdanau, D., Bougares, F., Schwenk, H., Bengio, Y.: Learning phrase representations using rnn encoder-decoder for statistical machine translation. arXiv preprint arXiv:1406.1078 (2014)
- [25] Vaswani, A., Shazeer, N., Parmar, N., Uszkoreit, J., Jones, L., Gomez, A.N., Kaiser, L., Polosukhin, I.: Attention is all you need. In: Advances

- in *Neural Information Processing Systems*, pp. 5998–6008 (2017)
- [26] Suhail, M., Mittal, A., Siddiquie, B., Broaddus, C., Eledath, J., Medioni, G., Sigal, L.: Energy-based learning for scene graph generation. In: *Proceedings of the IEEE/CVF Conference on Computer Vision and Pattern Recognition*, pp. 13936–13945 (2021)
- [27] Yang, J., Lu, J., Lee, S., Batra, D., Parikh, D.: Graph r-cnn for scene graph generation. In: *Proceedings of the European Conference on Computer Vision (ECCV)*, pp. 670–685 (2018)
- [28] Dai, B., Zhang, Y., Lin, D.: Detecting visual relationships with deep relational networks. In: *Proceedings of the IEEE Conference on Computer Vision and Pattern Recognition*, pp. 3076–3086 (2017)
- [29] Chen, T., Yu, W., Chen, R., Lin, L.: Knowledge-embedded routing network for scene graph generation. In: *Proceedings of the IEEE/CVF Conference on Computer Vision and Pattern Recognition*, pp. 6163–6171 (2019)
- [30] Tang, K., Zhang, H., Wu, B., Luo, W., Liu, W.: Learning to compose dynamic tree structures for visual contexts. In: *Proceedings of the IEEE/CVF Conference on Computer Vision and Pattern Recognition*, pp. 6619–6628 (2019)
- [31] Lu, C., Krishna, R., Bernstein, M., Fei-Fei, L.: Visual relationship detection with language priors. In: *European Conference on Computer Vision*, pp. 852–869 (2016). Springer
- [32] Zareian, A., Karaman, S., Chang, S.-F.: Bridging knowledge graphs to generate scene graphs. In: *European Conference on Computer Vision*, pp. 606–623 (2020). Springer
- [33] Zareian, A., Wang, Z., You, H., Chang, S.-F.: Learning visual common-sense for robust scene graph generation. In: *European Conference on Computer Vision*, pp. 642–657 (2020). Springer
- [34] He, K., Zhang, X., Ren, S., Sun, J.: Deep residual learning for image recognition. In: *Proceedings of the IEEE Conference on Computer Vision and Pattern Recognition*, pp. 770–778 (2016)
- [35] Lu, Y., Rai, H., Chang, J., Knyazev, B., Yu, G., Shekhar, S., Taylor, G.W., Volkovs, M.: Context-aware scene graph generation with seq2seq transformers
- [36] Krishna, R., Zhu, Y., Groth, O., Johnson, J., Hata, K., Kravitz, J., Chen,

- S., Kalantidis, Y., Li, L.-J., Shamma, D.A., *et al.*: Visual genome: Connecting language and vision using crowdsourced dense image annotations. *International journal of computer vision* **123**(1), 32–73 (2017)
- [37] Xu, D., Zhu, Y., Choy, C.B., Fei-Fei, L.: Scene graph generation by iterative message passing. In: *Proceedings of the IEEE Conference on Computer Vision and Pattern Recognition*, pp. 5410–5419 (2017)
- [38] Newell, A., Deng, J.: Pixels to graphs by associative embedding. *Advances in neural information processing systems* **30** (2017)
- [39] Ren, S., He, K., Girshick, R., Sun, J.: Faster r-cnn: Towards real-time object detection with region proposal networks. *Advances in neural information processing systems* **28** (2015)
- [40] He, K., Gkioxari, G., Dollár, P., Girshick, R.: Mask r-cnn. In: *Proceedings of the IEEE International Conference on Computer Vision*, pp. 2961–2969 (2017)
- [41] Pennington, J., Socher, R., Manning, C.D.: Glove: Global vectors for word representation. In: *Proceedings of the 2014 Conference on Empirical Methods in Natural Language Processing (EMNLP)*, pp. 1532–1543 (2014)